

Observation of electroweak W^+W^- pair production in association with two jets
in proton-proton collisions at $\sqrt{s} = 13$ TeV

—Supplemental Material—

The CMS Collaboration^a

^a*CERN, Geneva, Switzerland*

Abstract

Keywords: CMS, physics, VBS

Email address:

cms-publication-committee-chair@cern.ch (The CMS
Collaboration)

Preprint submitted to Elsevier

April 4, 2023

Table 1: Summary of the event categorization on top of signal candidates preselection. In each region, same-flavor final states share the same kinematic requirements.

Region	Final state	Requirements	Subregion
SR	$e\mu/\mu e$	$m_T > 60 \text{ GeV}$	$Z_{\ell\ell} < 1$
		$m_{\ell\ell} > 50 \text{ GeV}$	$Z_{\ell\ell} > 1$
		no b jet with $p_T > 20 \text{ GeV}$	
SR	ee	$m_{\ell\ell} > 120 \text{ GeV}$	$Z_{\ell\ell} < 1$
		$p_T^{\text{miss}} > 60 \text{ GeV}$	$Z_{\ell\ell} > 1$
SR	$\mu\mu$	no b jet with $p_T > 20 \text{ GeV}$	$Z_{\ell\ell} < 1$
			$Z_{\ell\ell} > 1$
$t\bar{t} + tW$ CR	$e\mu/\mu e$	$m_{\ell\ell} > 50 \text{ GeV}$	
		at least one b jet with $p_T > 20 \text{ GeV}$	
	ee	$m_{\ell\ell} > 120 \text{ GeV}$	
$t\bar{t} + tW$ CR		$p_T^{\text{miss}} > 60 \text{ GeV}$	
	$\mu\mu$	at least one b jet with $p_T > 20 \text{ GeV}$	
DY CR	$e\mu/\mu e$	$m_T < 60 \text{ GeV}$	
		$50 \text{ GeV} < m_{\ell\ell} < 80 \text{ GeV}$	
		no b jet with $p_T > 20 \text{ GeV}$	
DY CR	ee	$ m_{\ell\ell} - m_Z < 15 \text{ GeV}$	$ \Delta\eta_{jj} < 5$
		$p_T^{\text{miss}} > 60 \text{ GeV}$	$ \Delta\eta_{jj} > 5$
DY CR	$\mu\mu$	no b jet with $p_T > 20 \text{ GeV}$	$ \Delta\eta_{jj} < 5$
			$ \Delta\eta_{jj} > 5$

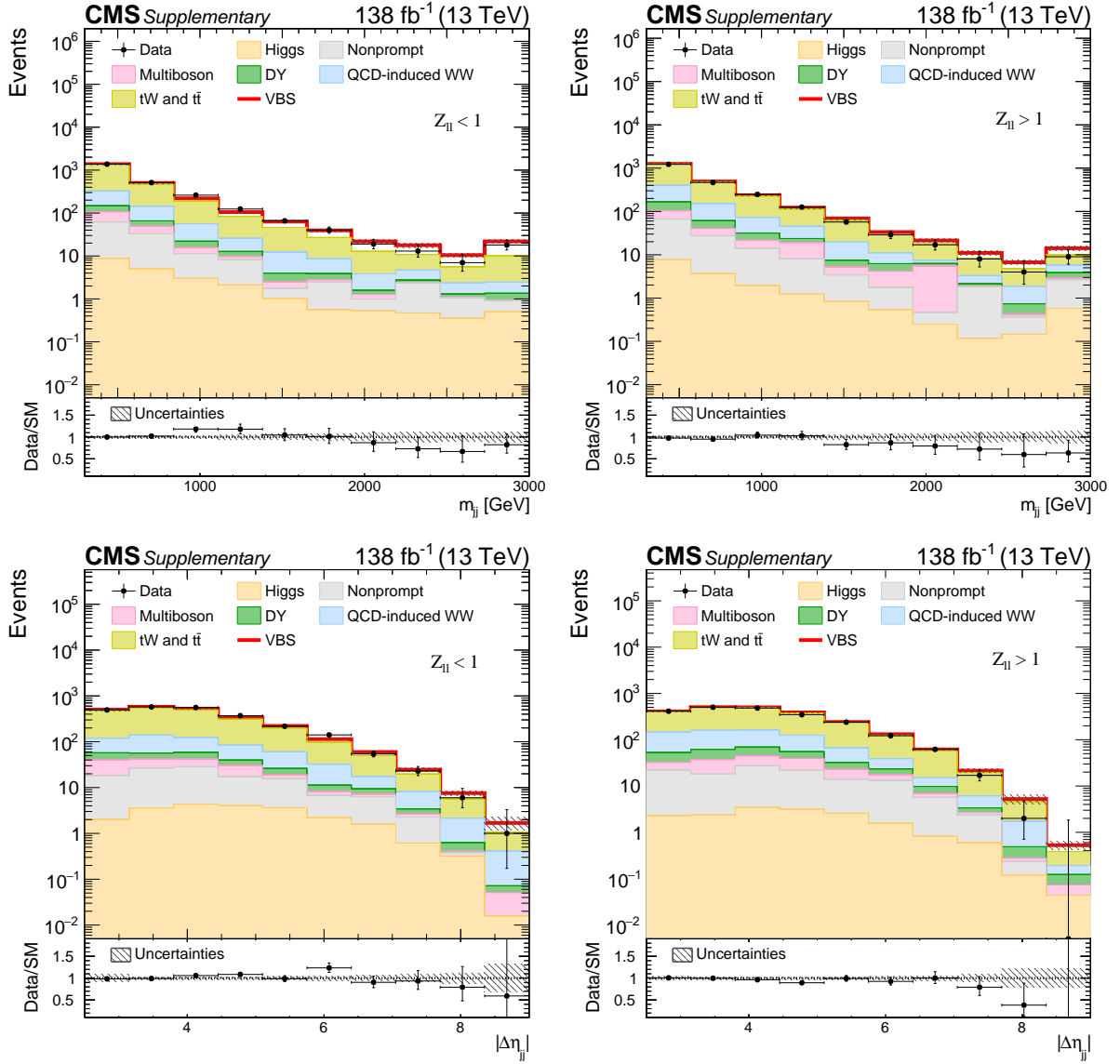


Figure 1: Post-fit distributions of m_{jj} (upper row) and $|\Delta\eta_{jj}|$ (lower row) variables in different-flavor SRs for $Z_{\ell\ell} < 1$ (left column) and $Z_{\ell\ell} > 1$ (right column) categories. These variables are among the nine observables used as inputs for the DNN, as listed in Table 2. The contributions from background and signal (red line) processes are shown as stacked histograms; systematic uncertainties are plotted as dashed gray bands. Data points are displayed with asymmetric Poisson vertical bars to ensure a correct statistical coverage all over the spectrum.

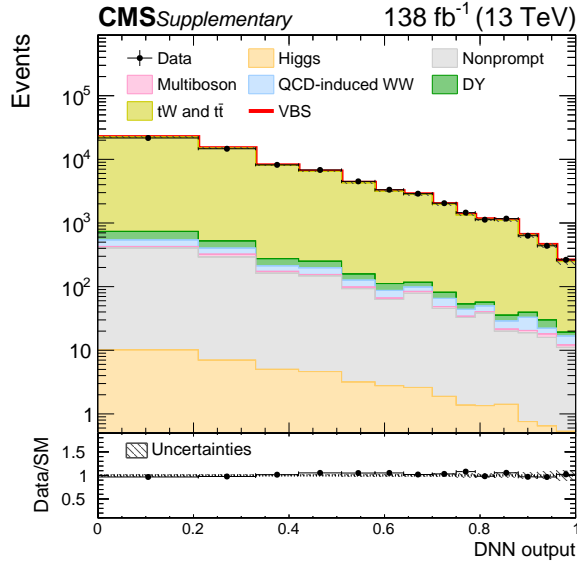


Figure 2: Post-fit distribution of the DNN output in different-flavor top CR. Data to SM expectation ratio has some residual shape dependence (less than 5% across the full spectrum), which however was found to not affect the analysis. The contributions from background and signal (red line) processes are shown as stacked histograms; systematic uncertainties are plotted as dashed gray bands. Data points are displayed with asymmetric Poisson vertical bars to ensure a correct statistical coverage all over the spectrum.

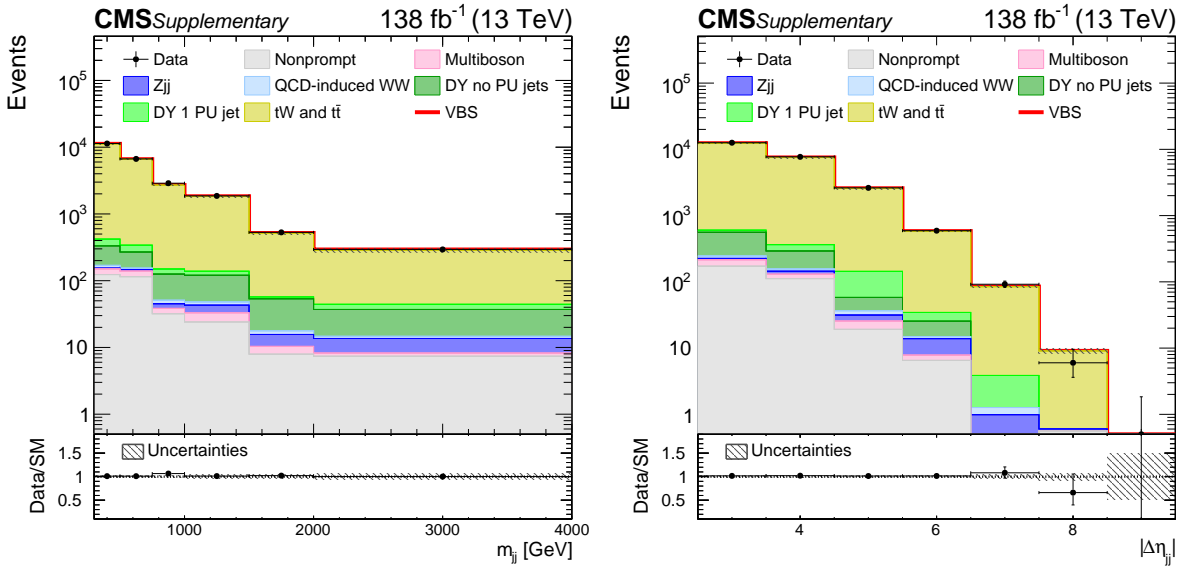


Figure 3: Post-fit distributions of m_{jj} (left) and $|\Delta\eta_{jj}|$ (right) variables in same-flavor top CR (ee and $\mu\mu$ final states combined). The ratio between data and SM expectation is in excellent agreement with 1 within post-fit uncertainties in both spectra. The contributions from background and signal (red line) processes are shown as stacked histograms; systematic uncertainties are plotted as dashed gray bands. Data points are displayed with asymmetric Poisson vertical bars to ensure a correct statistical coverage all over the spectrum.